

From HADES to PARADISE—atomistic simulation of defects in minerals

Stephen C Parker, David J Cooke, Sebastien Kerisit, Arnaud S Marmier, Sarah L Taylor and Stuart N Taylor

Department of Chemistry, University of Bath, Bath BA2 7AY, UK

E-mail: s.c.parker@bath.ac.uk

Received 20 November 2003

Published 25 June 2004

Online at stacks.iop.org/JPhysCM/16/S2735

doi:10.1088/0953-8984/16/27/010

Abstract

The development of the HADES code by Michael Norgett in the 1970s enabled, for the first time, the routine simulation of point defects in inorganic solids at the atomic scale. Using examples from current research we illustrate how the scope and applications of atomistic simulations have widened with time and yet still follow an approach readily identifiable with this early work. Firstly we discuss the use of the Mott–Littleton methodology to study the segregation of various isovalent cations to the (00.1) and (01.2) surfaces of haematite (α -Fe₂O₃). The results show that the size of the impurities has a considerable effect on the magnitude of the segregation energy. We then extend these simulations to investigate the effect of the concentration of the impurities at the surface on the segregation process using a supercell approach. We consider next the effect of segregation to stepped surfaces illustrating this with recent work on segregation of La³⁺ to CaF₂ surfaces, which show enhanced segregation to step edges. We discuss next the application of lattice dynamics to modelling point defects in complex oxide materials by applying this to the study of hydrogen incorporation into β -Mg₂SiO₄. Finally our attention is turned to a method for considering the surface energy of physically defective surfaces and we illustrate its approach by considering the low index surfaces of α -Al₂O₃.

(Some figures in this article are in colour only in the electronic version)

1. Introduction

In this paper we present some recent work using atomistic simulation techniques, which builds on the pioneering work of the AEA Theoretical Physics Group, at Harwell in the 1970s. We particularly pay tribute to the work of Michael Norgett in developing the HADES code [1, 2] and his emphasis on developing reliable interatomic potentials [3–5].

These interatomic potentials were based on the Born model of solids [6]. The short range interactions such as the electronic repulsion between the electron charge clouds on adjacent

atoms and then van der Waals forces were represented by simple, parametrized, analytical functions. The suggested functional form, called the Buckingham potential, is still employed by us today:

$$\Phi_{ij}(r_{ij}) = A_{ij} \exp(-r_{ij}/\rho_{ij}) - (C_{ij}/r_{ij}^6) \quad (1)$$

where Φ_{ij} is the short ranged interaction energy and A_{ij} , ρ_{ij} and C_{ij} are parameters specific to each pairwise interaction and r_{ij} is the separation between atom i and atom j .

Another achievement of those earlier simulations on inorganic solids was the recognition that in order to evaluate the structures and energies of defects reliably there must be some representation of the polarizability. Indeed the chosen model, i.e. the Dick and Overhauser shell model [7], continues to be the preferred choice for modelling the polarizability of the anion. In this approach the anions are represented by a core and massless shell, connected by a spring. These potential models have continued to enjoy success. In our group we have applied them to modelling the effects of pressure and temperature on the structures and stability of silicates [8, 9] and to investigating the stability of oxide interfaces [10–14].

In addition, the simulation codes we use are direct decedents of the HADES code and owe much to the work of Michael Norgett but have evolved to enable other properties to be evaluated. For example, METAPOCS (minimum energy techniques applied to the prediction of crystal structures) [15] was developed in the early 1980s and was designed to enable the study of materials periodic in three dimensions. Its energy minimization routines enabled both constant volume and constant pressure minimization to be undertaken. In the late 1980s and early 1990s the PARAPOCS (phonon assisted relaxations applied to the prediction of crystal structures) code was developed. It allowed the routine calculation of the free energy of inorganic materials using lattice dynamics [16, 17]. Currently our work is centred on the development and maintenance of the METADISE (minimum energy techniques applied to dislocations, interfaces and surface energies) [18] code. It uses the two-region approach also employed in the MIDAS code [19], which enables us to study a wide range of systems with different periodicities routinely. Perhaps therefore the ultimate challenge is to combine the functions of the latter two programs and develop a code that can undertake lattice dynamics calculations in systems with 1D and 2D periodicity thus achieving PARADISE (phonon assisted relaxations applied to dislocations, interfaces and surface energies).

This paper focuses on four topics of current research within our group. These illustrate that whilst the systems now considered were beyond the scope of the original HADES code the approaches are still based on the ideas it encapsulated and consequently owe much to the pioneering work of Michael Norgett and the Solid State Physics Group at AEA Harwell in the 1970s.

Firstly, we discuss the application of the Mott–Littleton [20] methodology, employed successfully within HADES, to study the segregation of various isovalent cations to the (00.1) and (01.2) surfaces of haematite (α -Fe₂O₃). We consider how the size of the impurity modifies the extent to which the impurity ions segregate to the stable low index surfaces. This is then extended using a supercell approach to consider the effect of the impurity concentration on the segregation process.

In addition to modelling the segregation to flat low index surfaces we consider segregation to one-dimensional defects at surfaces, and describe recent work on CaF₂ concerned with the segregation of La³⁺ at steps. The aim is to begin to investigate the effect of impurities on step growth. We then move beyond the simulation of defect energies by performing free energy minimization to study defect free energies in β -Mg₂SiO₄. Finally our attention is turned to a novel method for considering the energy of physically defective or non-stoichiometric surfaces. We illustrate the approach by considering the low index surfaces of α -Al₂O₃.

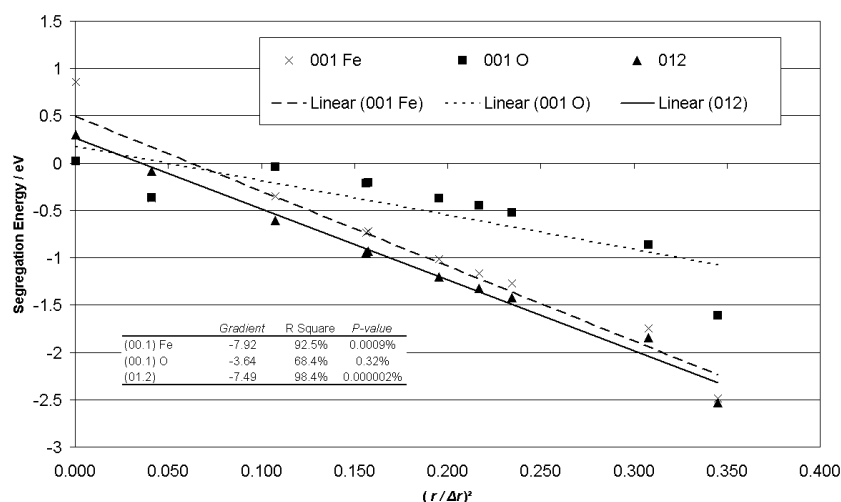


Figure 1. A plot of calculated segregation energy against relative impurity size for ten isovalent cations segregating to three dry surfaces of haematite considering only isolated defects.

2. Segregation to the low index surface of haematite

The HADES computer code was originally developed in order to automate the calculation of defects in bulk minerals. Leslie extended its functionality in the CASCADE code [21] and the methodology was applied to surfaces by Duffy and Tasker in the CHAOS code [22], which is now implemented in METADISE. Using these packages we have considered the segregation of isovalent impurities to two of the most stable low index surfaces of haematite (α -Fe₂O₃), namely the (00.1) and (01.2). In the case of the (00.1) surface an oxygen terminated surface was also considered in addition to the stable Fe terminated surface. The potential parameters used in the calculations were based on those derived by Lewis and Catlow [23].

Ten isovalent cations, namely Al³⁺, Cr³⁺, Eu³⁺, Gd³⁺, Ho³⁺, La³⁺, Lu³⁺, Nd³⁺, Tb³⁺ and Y³⁺, were chosen for study and each was substituted onto the surface replacing an Fe³⁺ ion. An equivalent calculation was also performed with the impurity in the bulk structure. The segregation energy is defined as the energy difference in incorporating an impurity at the surface compared to incorporating it into the bulk.

Intuitively we would expect the relative size of the impurity ion to have a bearing on the segregation process. Indeed, many segregation models have been proposed based on this supposition [24, 25]. One such model of segregation [26] states that the primary driving force for isovalent impurity segregation is the elastic strain, U_{elastic} , induced in the bulk lattice by the impurity. This is related to the difference in the size of the impurity and host cation, Δr , by equation (2):

$$U_{\text{elastic}} = \{(6\pi/r^3)(\Delta r/r)^2 B\}/\{1 + (3B/4\mu)\} \quad (2)$$

where r is the radius of the lattice cation (in this case Fe³⁺), B is the bulk modulus of the impurity and μ is the shear modulus of the host lattice. So if it is assumed that the bulk modulus is constant for all ten impurity ions then U_{elastic} , and hence the segregation energy, would be proportional to $(\Delta r/r)^2$.

The validity of this assumption has been tested by plotting the optimum segregation energy against the ratio $(\Delta r/r)^2$ and calculating the significance of the fit for each surface considered

and is shown graphically in figure 1. For all three surfaces the segregation energy is in general exothermic and therefore favoured energetically, there is also a clear relationship between the relative size of the impurity $(\Delta r/r)^2$ and the calculated segregation energy. Indeed formal statistical analysis reveals a highly significant correlation (significant at well in excess of the 0.01% confidence level in the case of the Fe terminated (00.1) surface and the (01.2) surface). The relationship is less significant for the oxygen terminated (00.1) surface where the largest and smallest cations show large deviations from the best-fit line. This behaviour is because the segregation energy is not independent of coverage and thus the isolated defect calculation does not represent the true optimum segregation energy for the system.

Departure from Langmuir behaviour is often observed when studying segregation effects [27]. One explanation for this is that as the concentration of impurity increases, there is an increase in the defect–defect interaction. Studies of alumina surfaces (α -Al₂O₃) determined that, for this mineral, the change in segregation energy with the concentration of impurity was non-linear [28]. Considering a number of surface configurations also enables symmetry effects and steric hindrance to be considered.

In order to go beyond isolated point defects and consider concentrations of impurity higher than the dilute limit, it is necessary to use a supercell approach. We scaled the surface unit cell so that there were six surface Fe³⁺ cations, which were then systematically substituted for each of the impurity cations. This enabled coverages in the range 16.67%–100% to be considered and thus determine whether Langmuir behaviour is followed and if the surface point defect represents the most stable concentration of impurity. These results are shown in figure 2.

In the case of the iron terminated surface the optimum coverage is still the isolated defect (equivalent to 0% coverage) considered previously. Thus accounting for the highly significant fit seen in figure 1 for this surface. This also suggests that segregation to this surface would only be observed when there is a large quantity of the impurity in the bulk structure.

Segregation energies at lower values than calculated for the point defect are predicted for the O terminated (00.1) surface. Figure 2 clearly illustrates that the segregation energy is not independent of coverage with distinct minima in the curves. This goes some way to explaining the poor fit seen in figure 1 and when the analysis is repeated with the calculated optimum segregation energies, the significance of the fit is dramatically improved (figure 3). The slope of the line is now calculated as being significant at the 0.000 03% significance level, illustrating a high probability that the relative size of the impurity ion is related to the magnitude of the segregation energy. Segregation at non-zero coverages of impurities has the effect of stabilizing the surface which in dry conditions has the highest surface energy of the three systems considered [29].

When only point defects were considered a highly significant (<0.000 01%) fit was found between the relative size of the impurity cation and the segregation energy for the (01.2) surface. Despite this, when the effect of concentration was considered, the minimum segregation was found to occur at 33.33% for all ten of the impurity ions. This concentration, also the optimum coverage for the O terminated (00.1) surface, is roughly equivalent to ratio of (Y³⁺ or Tb³⁺):Fe³⁺ in the well studied mixed oxide iron garnet (Fe₅X₈O₁₂ X = Y, Tb etc) materials previously studied using these potentials [30–32]. The change in segregation energy from that calculated for the isolated defect is however small (<0.3 eV), explaining why there is little improvement in the significance of the fit when the optimum segregation energy is plotted against $(\Delta r/r)^2$ figure 3. This small change in the segregation energy as the concentration is varied also leads to the prediction that a disordered surface would be observed.

In summary this work illustrates that whilst great insight can be gained into systems at the atomic level using the Mott–Littleton approach when considering surfaces, a greater understanding can be reached by considering the effect of defect concentration on the system

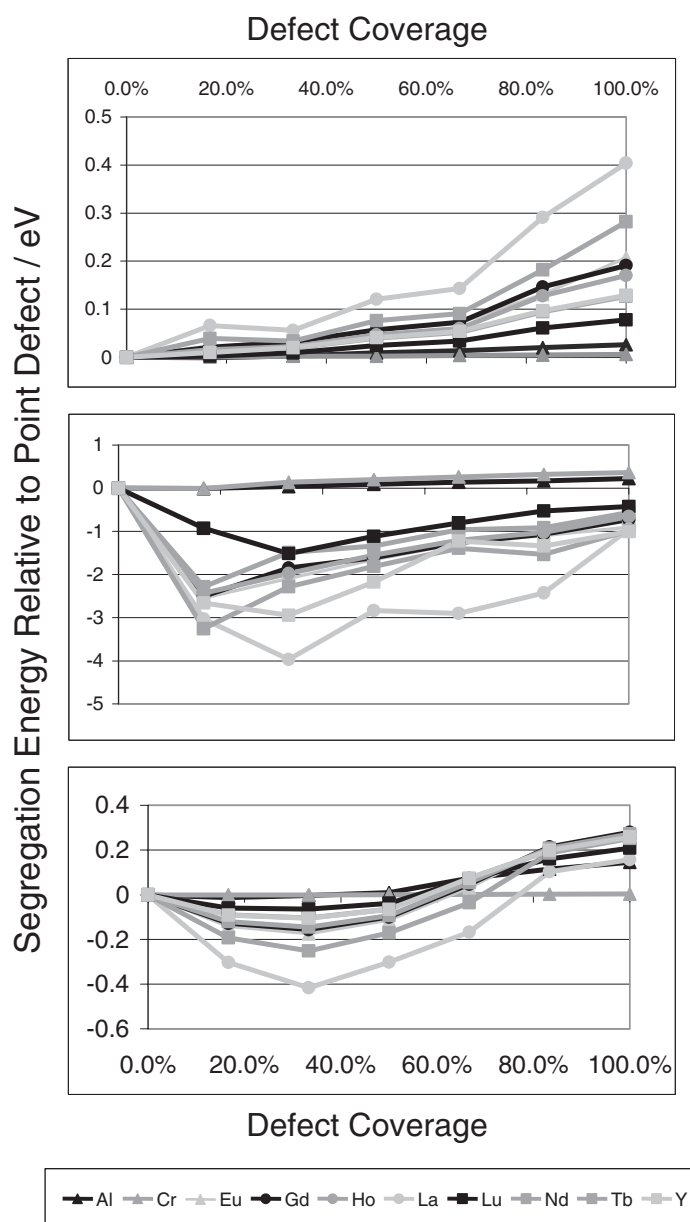


Figure 2. The effect of impurity coverage on segregation to the low index surfaces of haematite.

in question. This is examined in more detail in the next section when we consider the effect of lanthanum segregation on the dissolution of CaF_2 steps.

3. The effect of lanthanum defects at step sites of CaF_2

The atomistic simulation of CaF_2 is a topic particularly appropriate for inclusion in this paper paying tribute to the pioneering work of Norgett and the Theoretical Physics Division of the AEA Harwell Laboratory as this mineral [3] and equivalent alkaline-earth oxides [4] were

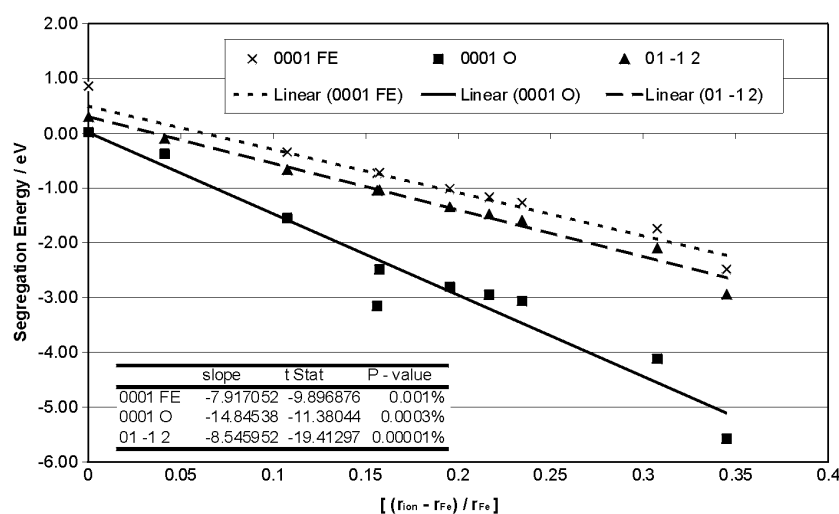


Figure 3. A plot of calculated segregation energy against relative impurity size for ten isoivalent cations segregating to three dry surfaces of haematite when the effect of surface coverage is considered.

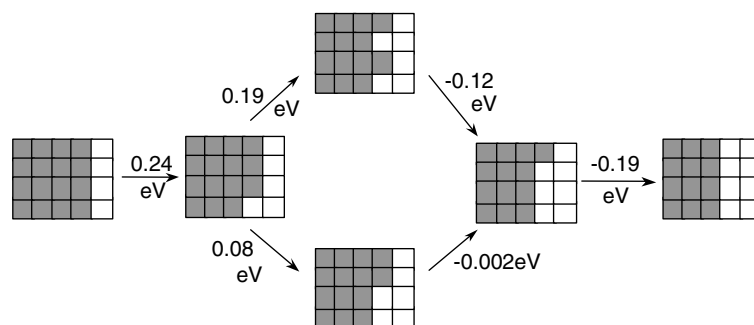


Figure 4. Energetics of the dissolution process. The steps correspond to the formation of the vacancy triplet of CaF_2 .

amongst the minerals studied by this group. Initially CaF_2 was studied as an analogue material to UO_2 [33] because the polycrystalline nature of uranium oxide made it difficult to characterize, which could be partially overcome by using high purity single crystals of CaF_2 . This early work was concerned with the study of ion interstitials in the bulk structure. Since then considerable research has extended the study of CaF_2 to include surfaces [34–36], molecular dynamics [11, 37] and electronic structure calculations [34, 38]. In this work we consider how the presence of La^{3+} affects the structure and stability of surface steps.

The potential parameters used were based on those derived by Catlow *et al* [5]. Our study began by optimizing the bulk structure at constant pressure before orientating the unit cell and cutting (140) surface. This plane was taken as a model growth surface as the step edges are far enough apart so that an impurity on one edge would not interact with an impurity on another. A supercell four unit cells wide was generated and energy minimized. CaF_2 units were then removed incrementally to gain the energy of dissolution of fluorite. This is the inverse of the growth process; therefore the energy required to add a unit to the face can be derived from this value.

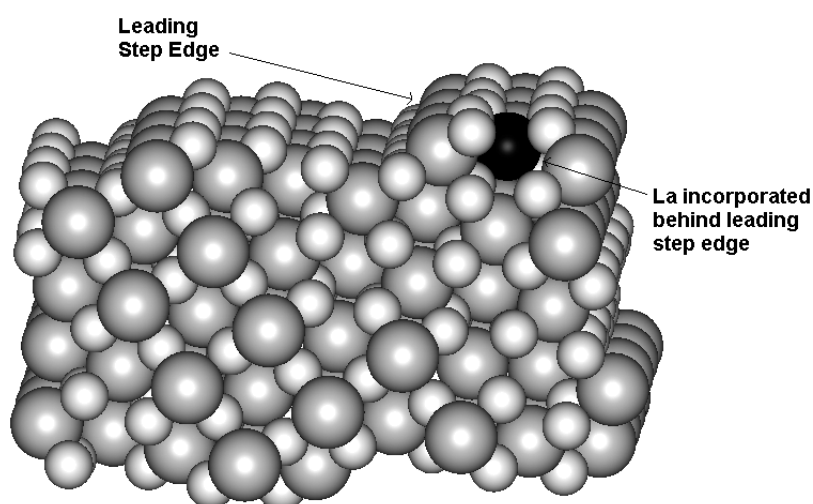
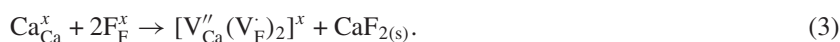


Figure 5. A CPK image of the step edge of a lanthanum substituted {140} slab.

The dissolution energy is defined as the energy to form the vacancy triplet and bulk CaF_2 :



The calculated results are shown in schematically in figure 4 and as expected the initial dissolution step is unfavourable, with the removal of the first vacancy cluster or CaF_2 unit, to the step edge having a positive value (+0.24 eV). However, the process becomes more favoured with the removal of subsequent units. The reverse process, involving growth of the step, follows the same trend beginning with the most positive energy (+0.19 eV). This is analogous to the previous work studying dissolution and growth at CaCO_3 steps [39] and is understandable; either the removal of a CaF_2 unit from a perfect step or the addition of a unit to a step gives rise to the largest change in number of the interactions. The figure also shows that on removal of material from the step that the energetically preferred route is to remove ions from the kink site rather than forming a new kink site.

Recent work by Dabrinhaus and Wandelt [36] simulated the adsorption of isolated CaF_2 molecules at flat and stepped surfaces and calculated an absolute adsorption energy of 5.05 eV. We can compare our energies directly by recalculating our energies by the difference in lattice energy and isolated molecular enthalpy. The individual adsorption energies range from 4.0 to 4.4 eV with an average dissociation energy of 4.19 eV relative to the isolated molecule. These compare well with the experimental sublimation enthalpy of 4.48 ± 0.09 eV at 298 K [40].

Previous studies on minerals other than fluorite, such as calcite [39], have indicated that the presence of impurities modify the mineral growth. Thus we considered the effect of lanthanum on the energetics of kink formation and hence on growth and dissolution. As lanthanum has a charge of +3, an additional fluoride ion was added to charge compensate the removal of calcium. In each case, when the location of the additional fluoride ion was varied, it preferred energetically to reside in the closest empty fluoride ion site to the lanthanum ion. Comparing the results in figures 4 and 6, it is clear that the greater binding energy of the lanthanum to the kink sites suggests that the steps will be decorated by lanthanum. In addition, if it is incorporated in a site adjacent to the step edge (figure 5), then the energy to move a vacancy at the step edge is increased. Thus increasing the energy required to dissolve a step edge. If the reverse process is considered then incorporating lanthanum to a completed step edge will cause additional calcium fluoride units adhering to that edge to bond preferentially at the

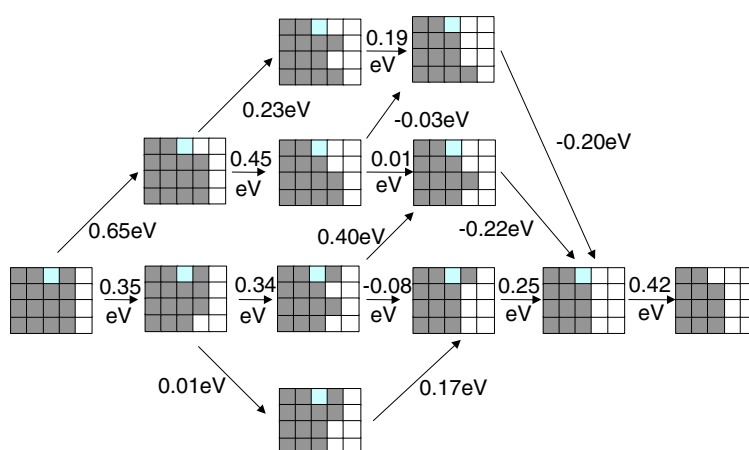


Figure 6. The dissolution scheme of the lanthanum substituted system, where the energies are those required to remove a mole of $\text{CaF}_2(\text{s})$.

site adjacent to the lanthanum. This reaction is favourable, with energy of -0.25 eV, while addition at a position not adjacent to the lanthanum incurs an energy penalty of the order of 0.2 eV. Having taken this preference into account, the growth scheme is similar to the non-doped step, with each subsequent CaF_2 adhering to the step edge immediately adjacent to any impurity already present. According to the scheme above, it appears perhaps unexpectedly, given trends in other materials, that lanthanum in fact acts to promote growth at the step edge.

In these first two examples the calculations have only considered the lattice energy of the crystal. In the next section however we demonstrate how it is possible to go beyond static lattice simulations and undertake free energy minimization using lattice dynamics.

4. Water defect in $\beta\text{-Mg}_2\text{SiO}_4$

One of the key unresolved questions in Earth sciences is to what extent is water present in the Earth's mantle. β -wadsleyite is one such mineral that has received significant attention due to its seemingly high water holding capacity [41]. Wadsleyite and ringwoodite were shown [42] to dissolve about an order of magnitude more water than polymorphs of MgSiO_3 (clinostatite, majorite and akimotoite) suggesting that the water content of the transition zone is likely to be far higher than that of the lower mantle. Partition coefficients estimated by Kawamoto *et al* [43] of water between these two phases and water suggest that wadsleyite is the most important host. Despite its potential importance, little at the atomic level is known because of the difficulty of investigating the trace amount of material at high pressures and temperatures. The aim of this work was, therefore, to use atomistic simulations to gain insight in the atomic structure of hypothetical defective structures of wadsleyite and to determine their ability to incorporate water.

We used the computer code PARAPOCS [16, 17] to perform free energy minimizations of the pure and defective wadsleyite structures. This approach was adopted because, unlike the calculations discussed previously, it enables us to consider minerals at temperatures and pressures similar to those found in the Earth's mantle. The potential parameters employed in this work were those derived by Lewis and Catlow [23], Saunders *et al* [44] and Baram and Parker [45]. Wadsleyite has cell dimensions of $a = 5.692$ Å, $b = 11.460$ Å, $c = 8.253$ Å and $\alpha = \beta = \gamma = 90^\circ$ at 1400°C and 16 GPa [46]. After constant pressure minimization at the same conditions the unit cell relaxed to $a = 5.581$ Å, $b = 11.251$ Å, $c = 8.138$ Å and

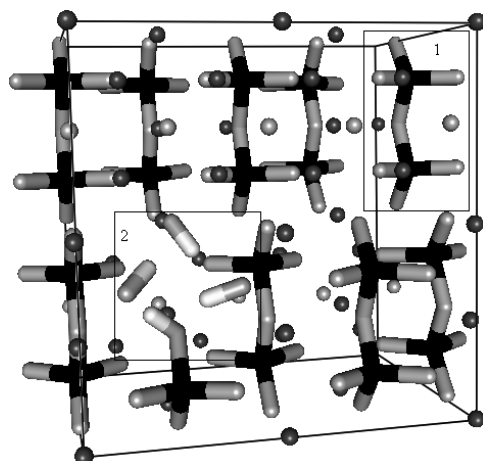
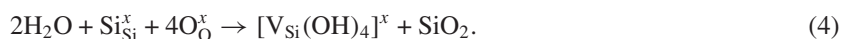


Figure 7. Wadsleyite structure, showing the $\text{Si}_2\text{O}_7^{6-}$ unit (1) and the hydrogarnet defect (2).

$\alpha = \beta = \gamma = 90^\circ$. The calculated cell dimensions are within 2% of the experimental values, which gives us confidence in our model.

Four types of defect were considered, namely hydrogarnet substitution, magnesium–hydrogen substitution, molecular water insertion and interstitial hydroxyl groups. The simulation cell was obtained by doubling the unit cell in the a direction and introducing one defect. This was done to reduce the defect concentration and to ensure that defects were separated by at least 8 Å. In addition, the simulation cell was sufficiently small to allow us to sample many hundreds of different configurations, which arise because there are four symmetry unrelated oxygen atom sites and three different magnesium sites and we also considered different pressures and temperatures. The calculations reported here were performed at 1900 K and 15 GPa, which was thought to be representative to the conditions in the transition zone.

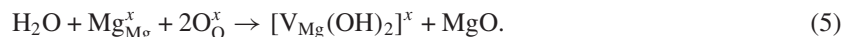
The hydrogarnet defect comprises a silicon vacancy and four hydrogen interstitials, protonating the four surrounding oxygen atoms, as shown in figure 7. Following the Kröger–Vink [47] defect notation, this reaction can be expressed as



We obtained a free energy of reaction of 1.15 eV. In the relaxed structure, the hydroxyl oxygen atoms occupy the oxygen sites and the hydrogen atoms lie along the tetrahedral faces and do not point directly towards the silicon vacancy as one might expect. Although the hydrogarnet defect is clearly important to several silicates, wadsleyite is unique with its arrangement of silicon and oxygen atoms. Rather than the typical SiO_4^{4-} tetrahedron, wadsleyite contains a bridging oxygen between two silicon atoms to form a $\text{Si}_2\text{O}_7^{6-}$ unit (see figure 7). This means that one of the four hydroxyl groups produced by the hydrogarnet substitution will come from a bridging oxygen and will therefore remain bonded to a silicon atom. The restriction on geometry for this hydroxyl group could account for the lower free energy of the hydrogarnet substitution in wadsleyite compared to other silicates. For example, Catlow and co-workers [48] calculated, for the hydrogarnet defect in grossular, an energy of reaction of 0.51 eV per water molecule. One of the alternative structures considered involved the protonation of the next O(1) along in the b direction instead of a O(2) bridging oxygen. The consequence was that all four hydroxyl groups had good orientational freedom. However, once relaxed, this structure was only marginally more stable and the free energy of reaction was only slightly lowered to

1.02 eV. In the relaxed structure, the three remaining hydroxyl groups lie with their hydrogen atom pointing towards the silicon vacancy.

A second defect considered involved substituting magnesium by hydrogen. The most stable is the neutral bound defect comprising a magnesium vacancy and two protonated neighbouring oxygen atoms. The reaction can be expressed as follows:



Substitutions of hydroxyls for O(1) oxygen atoms created the most stable structures. The configuration of lowest energy is obtained when a magnesium at a M(3) site is removed and two O(1) oxygen atoms are protonated with their hydrogen atoms directed at the magnesium vacancy. This gives a free energy of reaction of 0.64 eV. The O(1) protonation has been suggested several times as the most stable hydroxyl-containing structure [49, 50], but O(1) oxygen atoms represent only one eighth of the oxygen atoms in the unit cell. Half of the oxygen atoms are O(4) but reactions involving the protonation of these oxygens gives at best a free energy of reaction of 3.11 eV.

So far both substitutions resulted in the formation of hydroxyl groups but it has been suggested [4] that molecular water could also be formed in the crystal. In this case, a magnesium vacancy is created and two protons are added to the same oxygen atom to form a water molecule. The reaction can be written as



In the most stable structure, the vacancy is formed at a M(3) site and the two protons bond to a O(1) oxygen. The water molecule forms two hydrogen bonds with O(4) oxygen atoms from two different $\text{Si}_2\text{O}_7^{6-}$ units. Our predicted value for the free energy of reaction (3) is 2.4 eV.

Finally, the last substitution involved the formation of an oxygen vacancy and the addition of two hydroxyl groups in the vacancy vicinity. This reaction can be expressed as



We obtained a free energy of reaction of 3.00 eV, which is by far the least favoured reaction studied in this work. This reaction is not accompanied by the formation of a cation vacancy and thus probably suffers from a large energy penalty due to steric hindrance. In the most stable structure an O(3) oxygen is protonated and the insertion of a hydroxyl group a few ångströms away in the *a* direction causes the $\text{Si}_2\text{O}_7^{6-}$ unit to distort to a great extent.

In conclusion, we were able to use atomistic simulations together with lattice dynamics to successfully model the behaviour of minerals at different depths of the mantle. Also, our study predicts that water can be incorporated relatively easily in the wadsleyite structure at conditions relevant to the transition zone via the formation of a M3 magnesium vacancy and the protonation of two neighbouring O(1) oxygen atoms. If the same O(1) oxygen is protonated twice instead to form a water molecule which bridges two $\text{Si}_2\text{O}_7^{6-}$ units, the reaction is much more endothermic. Hydrogarnet substitution could also be a possible mechanism of incorporation of water in the lattice but the simple dissolution via interstitial hydroxyls is calculated to be highly unlikely. In the future, we want to investigate the effect of substituting Fe atoms at magnesium sites and see whether the reduction of Fe can help the dissolution of water in the crystal as it has been suggested by other groups [51–53].

5. Defective surfaces: an *ab initio* thermodynamic approach

The impressive developments both in raw computer power and in the algorithmic sophistication of codes have made not only bulk defects but also surface defects accessible to *ab initio* modelling. The *ab initio* modelling of defects is especially attractive, as the energy of a non-stoichiometric cell can be readily computed, while for ionic type potentials where particles

are often charged, different parametrizations can be required. Non-stoichiometry is especially relevant to surface sites, because these are obviously more accessible and more reactive than their bulk counterparts.

We have been using a method to compute the energy of periodically repeated defects at oxide surfaces (therefore non-stoichiometric), in equilibrium both with their bulk and with an atmosphere of gases at various temperature and partial pressures. This technique provides a good understanding of surface structures and stability, and under different conditions, whether ultrahigh vacuum, low temperature or natural environment.

Although the idea of using chemical potential to treat defects is far from new, its application to non-stoichiometric surfaces is more recent and has been popularized by the groups of Finnis [54] and Scheffler [55, 56].

We consider an oxide of chemical formula A_mO_n , in chemical equilibrium with an atmosphere containing O_2 , H_2 or H_2O , the oxide slab contains N_A metal atoms at chemical potential μ_A° , N_O oxygen atoms at chemical potential μ_O° and N_H hydrogen atoms at chemical potential μ_H° . The surface energy can be expressed as

$$\gamma_{AO} = \frac{1}{2S} (G_{AO}^{\text{slab}} - N_A \mu_A - N_O \mu_O - N_H \mu_H), \quad (8)$$

where G_{AO}^{slab} is the Gibbs free energy of the slab (of total surface area $2S$).

Defining the oxygen and hydrogen excesses, $\Gamma_O = [N_O/N_A] = \frac{1}{2S} (N_O - \frac{n}{m} N_A)$ and $\Gamma_H = [N_H/N_A] = \frac{1}{2S} (N_H)$, the Gibbs energy per formula unit, $g_{AO} = \frac{m}{N_A} G_{AO}^{\text{bulk}}$, using the fact that the surface is in equilibrium with its bulk, $g_{AO} = m\mu_A + n\mu_O$ and neglecting the entropic excess contributions to the free energy for the solids ($G_{AO}^{\text{slab}} \rightarrow E_{AO}^{\text{slab}}$ and $g_{AO} \rightarrow e_{AO}$), we can rewrite the surface energy as

$$\gamma_{AO} = \frac{1}{2S} \left(E_{AO}^{\text{slab}} - \frac{N_A}{m} e_{AO} \right) - \Gamma_O \mu_O - \Gamma_H \mu_H, \quad (9)$$

with stoichiometric and non-stoichiometric components.

We then subtract the surface energy of the most stable stoichiometric cut (acting as the reference phase):

$$\gamma_{AO}^{\text{defect}} = \gamma_{AO} - \gamma_{AO}^{\text{stoichio}} = \frac{1}{2S} (E_{AO}^{\text{slab}} - E_{AO}^{\text{stoichio}}) - \Gamma_O \mu_O - \Gamma_H \mu_H. \quad (10)$$

The above expression for the defect surface free energy is not very meaningful, as it does not ‘anchor’ the chemical potentials to physically relevant quantities. The chemical potentials are bounded: for μ_A lower than μ_A^{metal} the oxide will dissociate, while at high μ_O molecular O_2 would start to condense at the surface. These conditions lead to

$$\frac{g_{AO} - m g_A}{n} < \mu_O < \frac{1}{2} g_{O_2}, \quad (11)$$

where the Gibbs energy per formula unit g_A is taken as the calculated energy of the bulk metal e_A (here again assuming that the entropic contribution is negligible—which is reasonable for solids), and g_{O_2} is the Gibbs energy of an isolated O_2 molecule (at the temperature of interest). Evaluating the Gibbs energy of the O_2 molecule can therefore complete this boundary calculation. However, there are a few caveats, as the energy of the O_2 molecule is poorly reproduced by DFT and it is not possible to neglect the vibrational terms for gases. Using the formation cycle of the oxide and tabulated thermodynamical data [57] solves these difficulties.

The chemical potential of O, assuming an ideal gas, is $\mu_O = \mu_O^\circ(T) + \frac{1}{2} k T \log(\frac{P_{O_2}}{P^\circ})$ and for a given value of μ_O one can extract the partial pressure knowing the temperature, or vice versa. The same can be done for H, but the expression to use depends whether the surface hydrogen is in equilibrium with H_2 or H_2O .

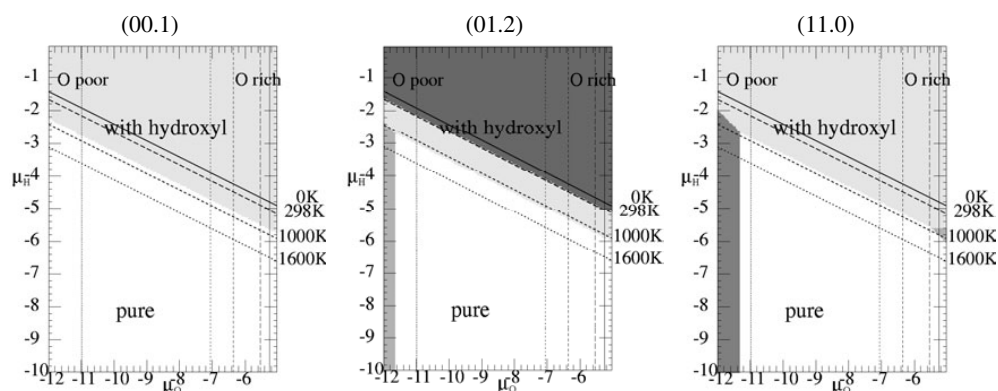


Figure 8. Phase diagrams for alumina surfaces (chemical potential in eV).

Table 1. Surfaces energies of alumina, absolute and relative to the (00.1) surface.

Face	Area	Experiment [5] (relative)	Experiment [6] (relative)	DFT-GGA			
				this work (J m ⁻² , relative)		DFT-LDA [9] (J m ⁻² , relative)	
(00.1)	19.53	1.00	1.00	1.94	1.00	1.76	1.00
(01.2)	24.27	0.85	1.05	2.04	1.03	1.97	1.12
(11.3)	40.50	0.96	1.06	2.25	1.13	—	—
(11.0)	35.49	0.97	1.12	2.34	1.18	1.86	1.06
(10.0)	61.46	1.01	1.16	2.56	1.29	1.40	0.80
(10.1)	20.49	0.95	1.07	2.56	1.29	2.55	1.45

To summarize the procedure: the energy of slabs supporting different periodic defects are calculated (and stoichiometric slab and corresponding bulk), a phase diagram is constructed from equation (10), as well as the correspondence between (μ_O, μ_H) and $(T, P_{O_2}, P_{H_2}, P_{H_2O})$ (from experimental data and the calculated energies of hydrogen and water molecules and bulk metal).

We applied this technique to the surfaces of alumina. While the basal surface of this crystal has been studied intensively due to a discrepancy between experiment and modelling, the other surfaces have been neglected. Recent morphology [58, 59] and structural experiment [60, 61] are offering data on other surfaces ((01.2) and (11.0)), and an opportunity to better understand the origin of the disagreement between experimental and theoretical results concerning the basal plane. We calculated the energy of slabs of different stoichiometry constructed to model the six surfaces appearing in the morphology experiments ((00.1), (01.2), (11.3), (11.0), (10.0) and (10.1)).

To start, we compare the energy of the stoichiometric surfaces in table 1.

With the exception of the (10.1) surface (and surprisingly the (00.1) in the case of Choi and co-workers [58]), the experimental and theoretical ordering of surface energy compares well. Considering the lack of structural experiment on the (10.1) surface, the possible explanations are that it could either be stabilized by faceting (reducing the surface energy) or adopts a different stoichiometry. We then construct the phase diagrams for each surface. We considered Al and O vacancies, as well as O, H, OH and H₂O adsorption.

In figure 8, we show the phase diagrams corresponding to three surfaces which have been studied by structure sensitive probes. The most important result from the surface phase diagram

of figure 8 is that only two types of surfaces can be found on alumina: pure (stoichiometric) or hydroxylated. Also, the hydroxylated surfaces are those where the Al are sixfold coordinated and the O threefold coordinated. Thus the surfaces are formed by the addition of a few water molecules per unit cell to the stoichiometric surface, which results in the boundary between the two phases being parallel to the hydrogen/water equilibrium. In the case of the basal surface (00.1) the structure of the hydroxylated surfaces, minus its hydrogen, corresponds to the ‘oxygen terminated’ surface evidenced by some experiments [62].

Furthermore, the two best candidates for the (01.2) surface, as observed by crystal truncation rod diffraction [60], were the stoichiometric and an oxygen terminated surface, which with additional hydrogen corresponds to the fully hydroxylated surface we observe. This surface is especially interesting as two different hydroxylated surfaces appear. The first one corresponds to the hydroxylation of the most stable cut, with two water molecules per unit area, while the second results from the hydroxylation of another cut of the surface, significantly less stable than the most stable one, by 2.5 J m^{-2} , but which allows three water molecules to dissociate and bond. It is this last structure, favoured at higher water chemical potential, which corresponds to the CTRD best fit.

Taking into account the fact that hydrogen is notoriously difficult to observe with LEED and CTRD, we conclude that the oxygen terminated surfaces are indeed not very stable, but that these hydroxylated surfaces which allow the Al to be sixfold coordinated and the O to be threefold coordinated definitely are, under realistic conditions. At higher temperature, or very low partial pressures, the non-defective surfaces should be more stable.

6. Conclusion and scope for future work

We have illustrated, using some examples of our current work, how we owe much to and follow the same philosophy as those methods developed in the Theoretical Physics Group at Harwell in the 1970s, implemented in the HADES code by Michael Norgett. The legacy of high quality simulation codes and the emphasis on the care that must be taken in using and developing potential models describing the interatomic potentials has enabled us to continue extending the work.

One of the areas that has been expanded, thanks also to the increase in computational resources, has been the ability to more effectively search configurational space. For example, the work on segregation of isovalent impurities to haematite surfaces shows that the type of impurity, surface and surface concentration can all be varied. The results show that the segregation energy varies significantly as a function of coverage. The work on the formation of neutral vacancy clusters at the steps of calcium fluoride suggests that lanthanum will tend to decorate the steps and both increase the energetic favourability of growing the step and also reducing the dissolution. A further extension has been to be able to incorporate the effects of high pressures and temperatures. By using free energy minimization methods we were able to model the incorporation of water in wadsleyite, which is thought to have a high water storage, at temperatures and pressures relevant to the transition zone of the Earth’s mantle. We studied four possible types of defects and found that the formation of a M3 magnesium vacancy and the protonation of two neighbouring O(1) oxygen atoms is the most energetically favoured way of introducing water in the structure. Finally, the study of defects in polar solids is now being addressed by *ab initio* techniques. We describe modelling of defective surfaces of oxides. Phase diagrams were produced for different surfaces of α -alumina, which then allow the determination of the thermodynamically most stable configuration under a set of experimental conditions of pressure and temperatures. It was shown that, in an atmosphere containing H_2 , O_2 and H_2O , only non-defective (stoichiometric) or hydroxylated surfaces

were thermodynamically stable, and that in the case of the (01.2) surface, the most stable hydroxylated surface originated from a different cut than the most stable non-defective surface.

Finally, our aim for the future is to develop a method of incorporating one- and two-dimensional periodicity into lattice dynamics, which if successful would enable us to have truly moved from HADES to PARADISE.

Acknowledgments

We would like to acknowledge the NERC e-science initiative and EPSRC grants GR/H0413 and GR/H0185 for funding and additionally HEFCE grant JREI JR99BAPAEQ for the provision of computer time.

References

- [1] Norgett M J 1974 A general formulation of the problem of calculating the energies of lattice defects in ionic crystals *Atomic Energy Research Establishment, Harwell R.7650 HL74/335*
- [2] Norgett M J 1972 A users guide to HADES *Atomic Energy Research Establishment, Harwell R.7015 HL72/550*
- [3] Norgett M J 1971 *J. Phys. C: Solid State Phys.* **4** 298
- [4] Norgett M J 1971 *J. Phys. C: Solid State Phys.* **4** 1284
- [5] Catlow C R A, Norgett M J and Ross T A 1977 *J. Phys. C: Solid State Phys.* **10** 1627
- [6] Born M and Huang K 1954 *Dynamical Theory of Crystal Lattices* (Oxford: Oxford University Press)
- [7] Dick B G and Overhauser A W 1958 *Phys. Rev.* **112** 90
- [8] Vocadlo L *et al* 1995 *Phys. Earth Planet. Inter.* **88** 193
- [9] Couves J W *et al* 1993 *J. Phys.: Condens. Matter* **5** L329
- [10] Oliver P M, Watson G W and Parker S C 1995 *Phys. Rev. B* **52** 5323
- [11] de Leeuw N H and Parker S C 1997 *J. Chem. Soc. Faraday Trans.* **93** 467
- [12] de Leeuw N H and Parker S C 1998 *Phys. Rev. B* **58** 13901
- [13] Higgins F W, Watson G W and Parker S C 1997 *J. Phys. Chem.* **101** 9964
- [14] Parker S C *et al* 2001 *Molecular Modeling Theory: Applications in the Geosciences (MSA, 2001)* vol 42, ed R T Cygan and J D Kubicki (Washington, DC: The Mineralogical Society of America) p 63
- [15] Parker S C 1982 *Chemistry* (London: University of London)
- [16] Watson G W *et al* 1997 *Computer Modelling in Inorganic Crystallography* ed C R A Catlow (New York: Academic) p 55
- [17] Parker S C and Price G D 1989 *Adv. Solid State Chem.* **1** 295
- [18] Watson G W *et al* 1996 *J. Chem. Soc. Faraday Trans.* **92** 433
- [19] Tasker P W 1978 *AERE Technical Report* R9130
- [20] Mott N and Littleton M 1938 *Trans. Faraday Soc.* **38** 485
- [21] Leslie M 1982 *SERC Daresbury AERE Report* AERE R11059
- [22] Duffy D M and Tasker P W 1983 *Harwell Technical Report* AERE R11059
- [23] Lewis G V and Catlow C R A 1985 *J. Phys. C: Solid State Phys.* **18** 1149
- [24] Davies M J *et al* 1989 *J. Chem. Soc. Faraday Trans.* **85** 555
- [25] Davies M J 1992 *PhD Thesis* University of Bath
- [26] McLean D 1957 *Grain Boundaries in Metals* (London: Clarendon)
- [27] Sayle T X T, Parker S C and Catlow C R A 1994 *J. Phys. Chem.* **98** 13625
- [28] Kenway P R, Parker S C and Mackrodt W C 1989 *Mol. Simul.* **4** 175
- [29] Parker S C, de Leeuw N H and Redfern S E 1999 *Faraday Discuss.* **114** 381
- [30] Saunders G A *et al* 1992 *Phys. Rev. B* **46** 8756
- [31] Donnerberg H and Catlow C R A 1993 *J. Phys.: Condens. Matter* **5** 2947
- [32] Donnerberg H and Catlow C R A 1994 *Phys. Rev. B* **50** 744
- [33] Norgett M J and Lidiard A B 1968 *Phil. Mag.* **18** 1193
- [34] de Leeuw N H and Cooper T G 2003 *J. Mater. Chem.* **13** 93
- [35] Vyas S *et al* 2001 *Mol. Simul.* **26** 307
- [36] Dabringhaus H and Wandelt K 2003 *Surf. Sci.* **526** 257
- [37] de Leeuw N H, Parker S C and Rao K H 1998 *Langmuir* **14** 5900
- [38] de Leeuw N H *et al* 2000 *Surf. Sci.* **452** 9

- [39] de Leeuw N H, Parker S C and Harding J H 1999 *Phys. Rev. B* **60** 13792
- [40] Blue G D *et al* 1967 *J. Phys. Chem.* **67** 877
- [41] Kohlstedt D L, Keppeler H and Rubie D C 1996 *Contrib. Mineral. Petrol.* **123** 345
- [42] Ohtani E *et al* 2001 *Phys. Earth Planet. Inter.* **124** 105
- [43] Kawamoto T, Hervig R L and Holloway J R 1996 *Earth Planet. Sci. Lett.* **142** 587
- [44] Sanders M J, Leslie M and Catlow C R A 1984 *J. Chem. Soc. Chem. Commun.* 1271
- [45] Baram P S and Parker S C 1996 *Phil. Mag. B* **73** 49
- [46] Finger L W *et al* 1993 *Phys. Chem. Minerals* **19** 361
- [47] Kröger F A 1972 *The Chemistry of Imperfect Crystals* (Amsterdam: North-Holland)
- [48] Wright K, Freer R and Catlow C R A 1994 *Phys. Chem. Minerals* **20** 500
- [49] Smyth J R 1987 *Am. Mineral.* **72** 1051
- [50] Haiber M, Ballone P and Parrinello M 1997 *Am. Mineral.* **82** 913
- [51] Ingrin J and Skogby H 2000 *Eur. J. Mineral.* **12** 543
- [52] Wright K and Catlow C R A 1994 *Phys. Chem. Minerals* **20** 515
- [53] Wright K and Catlow C R A 1996 *Phys. Chem. Minerals* **23** 38
- [54] Batirev I G *et al* 1999 *Phys. Rev. Lett.* **82** 1510
- [55] Wang X G *et al* 1998 *Phys. Rev. Lett.* **81** 1038
- [56] Reuter K and Scheffler M 2002 *Phys. Rev. B* **65** 035406
- [57] Afeefy H Y, Liebman J F and Stein S E 2003 *NIST Chemistry WebBook (NIST Standard Reference Database Number vol 69)* ed P J Linstrom and W G Mallard (Gaithersburg, MD: National Institute of Standards and Technology)
- [58] Choi J H *et al* 1997 *J. Am. Ceram. Soc.* **80** 62
- [59] Kitayama M and Glaeser A M 2002 *J. Am. Ceram. Soc.* **85** 611
- [60] Trainor T P *et al* 2002 *Surf. Sci.* **496** 238
- [61] Becker T *et al* 2002 *Phys. Rev. B* **65** 115401
- [62] Toofan J and Watson P R 1998 *Surf. Sci.* **401** 162